Current Biology, Volume *30*

Supplemental Information

Transient Disruption of the
Inferior Parietal Lobule Impairs the Ability
to Attribute Intention to Action

Jean-François Patri, Andrea Cavallo, Kiri Pullar, Marco Soriano, Martina Valente, Atesh Koul, Alessio Avenanti, Stefano Panzeri, and Cristina Becchio

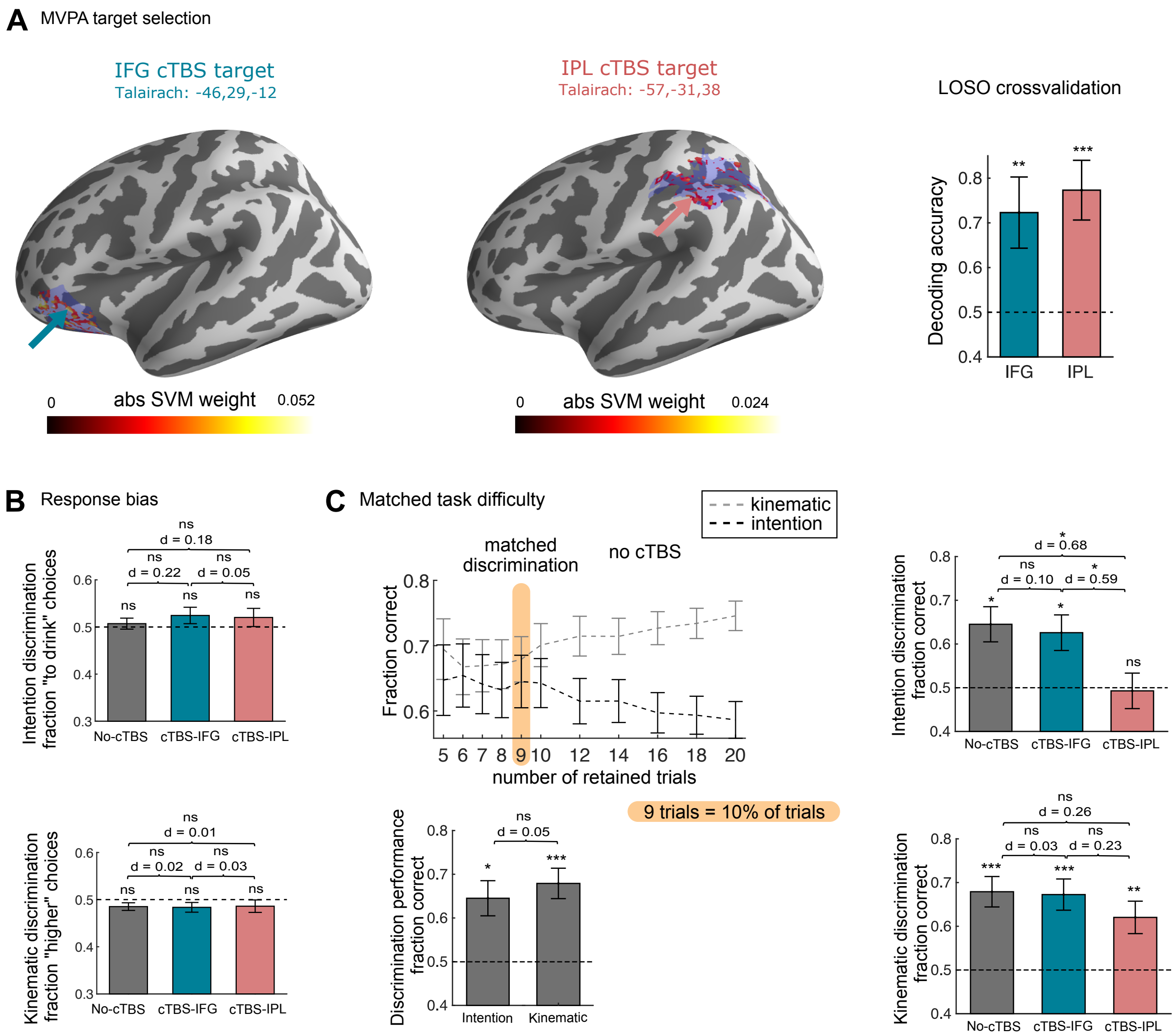

Figure S1. Experimental design and further analyses of behavioral discrimination performance. Related to Figure 1. (A) Target sites of cTBS in the left IFG pars orbitalis and the left IPL anterior. Regions in slate blue indicate ROIs included in linear SVM classifier fitting. Cortical surface projections of the 20% highest ranked voxels for classifying intention in the left IFG pars orbitalis and left IPL are displayed. The figure displays the absolute values of weights averaged over LOSO cross validation folds. Arrows indicate the coordinates chosen for cTBS. **(B)** Fraction of 'to drink' answers in the intention discrimination task and 'higher' answers in the kinematic discrimination task in each experimental session. Results are reported as mean ± SEM across subjects. **(C)** Control analyses with matched discrimination performance. (Left) Discrimination performance as a function of the number of retained trials. Orange area indicates the 10% level trial selection. With this selection, discrimination performance did not differ between the two tasks in no cTBS (two proportion z test: z = -0.61, Cohen's d = -0.05, p = 0.42). (Right) Discrimination performance (fraction correct) in the intention discrimination task and in the kinematic discrimination task with 10% level trial selection. Histograms represent mean ± SEM across participants. Cohen's effect size (d) for each comparison is reported.

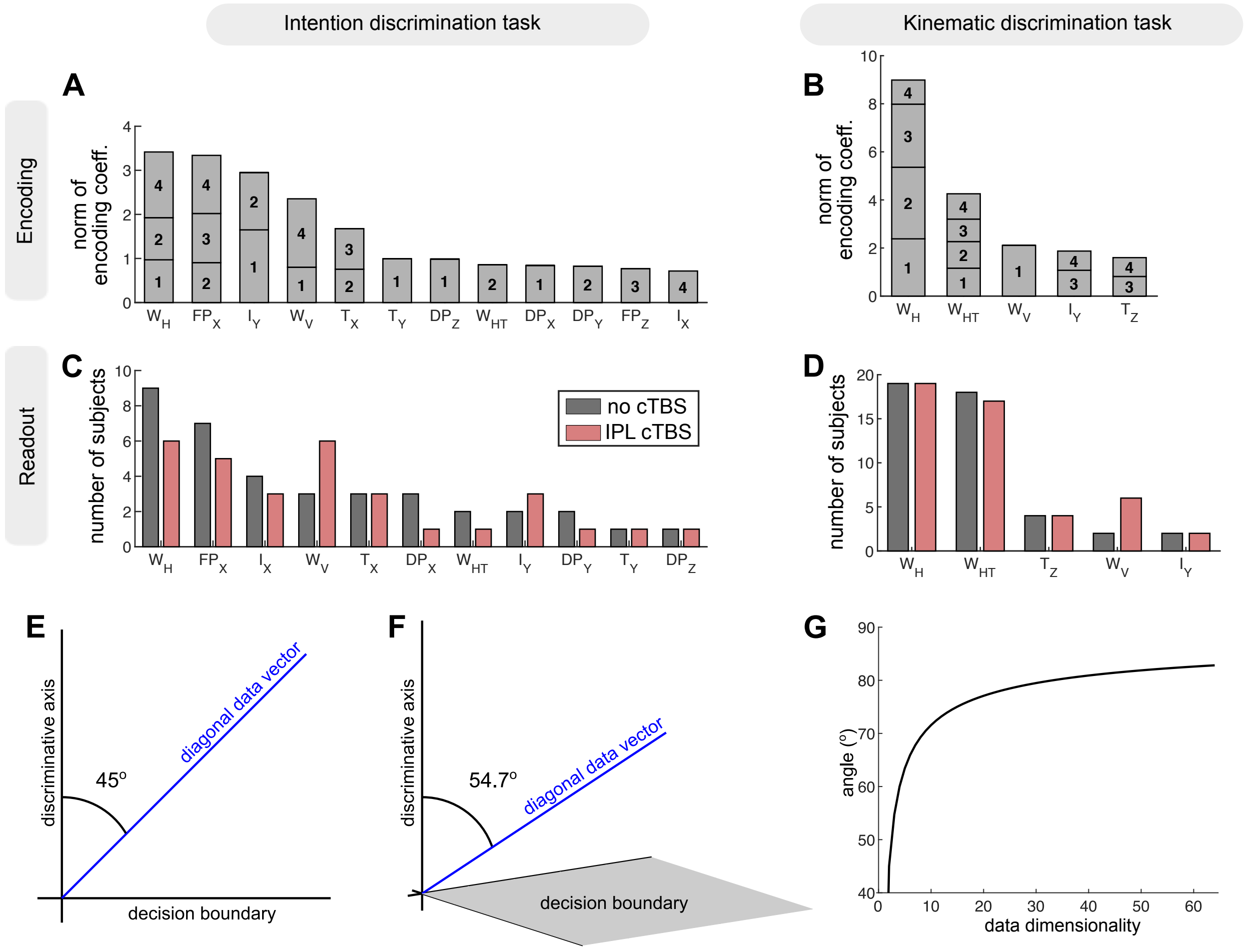

Figure S2. Encoding and readout models and angles. Related to Figure 2. Panels (A)-(D) report the ranking of features with respect to encoding and readout. **(A)-(B)** Sum of the absolute value of encoding regression coefficients over time bins encoding significant intention **(A)** and wrist height **(B)** discriminative information. Features are ordered left to right from most informative to least informative. **(C)-(D)** Number of observers who read out a specific variable in any of the time bins in the intention discrimination task **(C)** and in the kinematic discrimination task **(D)**. Features are ordered left to right from most to least readout. **(E)-(G)** Encoding and readout angles in high-dimensional kinematic feature space. In high-dimensional spaces, mean angles tend to fall in a region of space that gets closer and closer to orthogonality as dimensionality increases. **(E)** In a 2-dimensional space, the decision boundary is a 1-dimensional line, and a diagonal vector in which the component along the discriminative axis (i.e., the axis orthogonal to the decision boundary) equals the components along the non-discriminative axis (i.e., axis parallel to the decision boundary) lies on a 45° angle. **(F)** In a 3-dimensional space, the decision boundary is a 2 dimensional hyperplane, and the diagonal vector lies at an angle of 54.7° from the discriminative axis. **(G)** Value of the angle of the diagonal vector plotted as a function of the dimension of the feature space. In n-dimensional space, a diagonal vector in which the component along the discriminative axis (i.e., axis orthogonal to the decision boundary) equals the components along the non-discriminative axes (i.e., axes parallel to the n-1 dimensional decision hyperplane) corresponds to an arccos (1/sqrt(n)) angle from the discriminative axis. This corresponds to 82.7° in a 64-dimensional space such as the one used for our readout and encoding models.

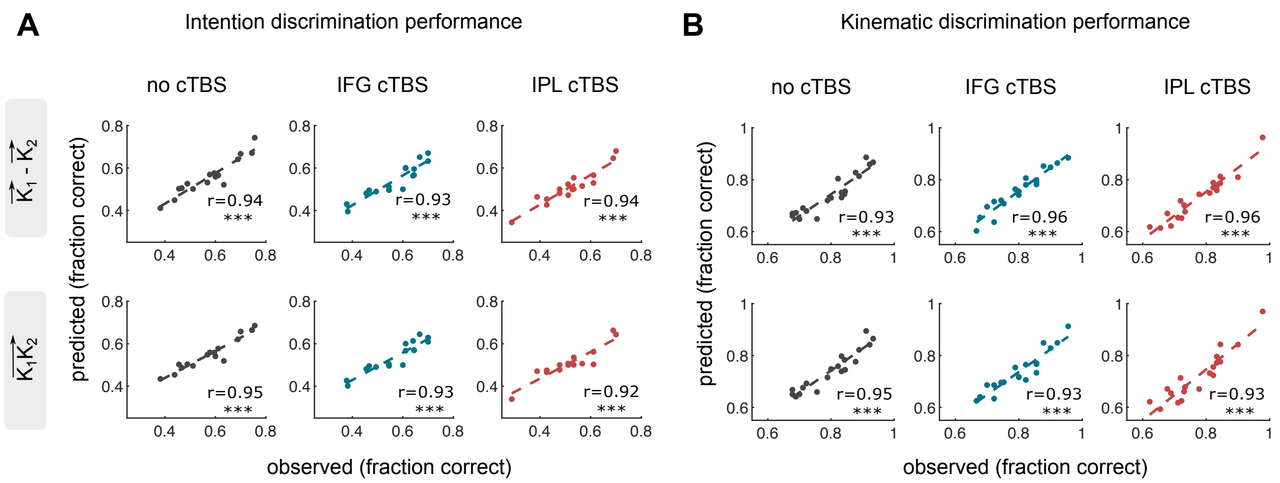

Figure S3. Comparison between models using the difference in kinematic features and models using all the kinematic features of the two reach-to-grasp acts. Related to Figure 3. We assessed whether a more complex readout model, using the full set of kinematic features of the first and second grasping act independently (that is, $\vec{K} = [\vec{K_1}, \vec{K_2}]$), rather than their difference, would achieve better performance. The same regularization procedure, described in STAR Methods was applied. Scatterplots of the relationship between the observed and predicted discrimination performance across individual participants are reported for the intention discrimination task **(A)** and the kinematic discrimination task **(B).** For the intention discrimination task, the model using the full set of kinematic features did not perform better than the model using the difference in kinematics in any of the sessions ($p > 0.4$ using LMEM). For the kinematic discrimination task, the model using the full set of features showed a small advantage for no cTBS and IPL cTBS sessions (model performance as fraction correct: 0.88 vs 0.91, $p = 0.012$ for no cTBS, 0.88 vs 0.90 $p = 0.044$ for IPL cTBS). Both approaches achieved similarly high correlations between predicted and observed task performance ($p < 0.001$ in all cases).

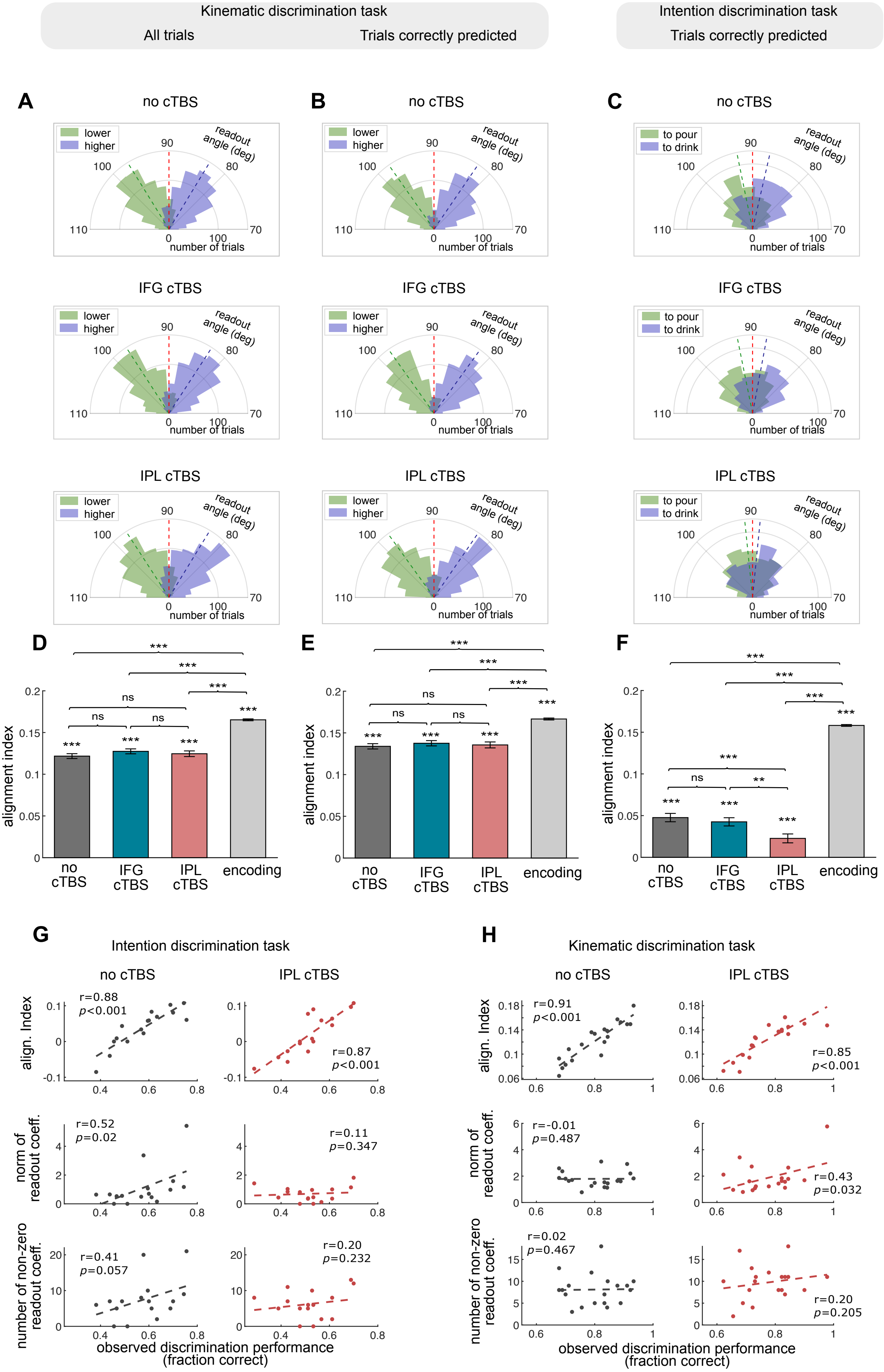

Kinematic discrimination task
All trials
Trials correctly predicted
Intention discrimination task
Trials correctly predicted
A
B
C
no cTBS
IFG cTBS
IPL cTBS
lower
higher
to pour
to drink
readout angle (deg)
90
80
70
100
110
0
100
number of trials
D
E
F
alignment index
0
0.05
0.1
0.15
0.2
***
**
ns
no cTBS
IFG cTBS
IPL cTBS
encoding
G
Intention discrimination task
H
Kinematic discrimination task
align. Index
norm of readout coeff.
number of non-zero readout coeff.
observed discrimination performance (fraction correct)
r=0.88
p<0.001
r=0.87
p<0.001
r=0.52
p=0.02
r=0.11
p=0.347
r=0.41
p=0.057
r=0.20
p=0.232
r=0.91
p<0.001
r=0.85
p<0.001
r=-0.01
p=0.487
r=0.43
p=0.032
r=0.02
p=0.467
r=0.20
p=0.205

Figure S4. Additional analyses on the effect of cTBS on alignment. Related to Figure 4. (A)-(B) Polar distribution of readout angles in the kinematic discrimination task under no cTBS, IFG cTBS and IPL cTBS. Panel **(A)** reports results for all trials. Panel **(B)** reports results for trials correctly predicted by the model only. **(C)** Polar distribution of readout angles in the intention discrimination task under no cTBS, IFG cTBS and IPL cTBS considering trials correctly predicted by the model only. For graphical representation, in panels **(A)-(C**), the 70-110° angle range of polar distributions is expanded to a semi-circle. The dashed red line marks the readout boundary (90°). **(D)-(E)** Effect of cTBS on the alignment index the kinematic discrimination task. Panel **(D)** reports results for all trials. Panel **(E)** reports results for trials correctly predicted by the model only. **(F)** Effect of cTBS on the alignment index the intention discrimination task considering trials correctly predicted by the model only. In panels **(D)-(F),** the value of the alignment index of the encoding angle is also reported for comparison. Histograms represent mean ± SEM across all trials and participants. **(G)-(H)** Scatterplots of the alignment index, the norm of readout vector and the number of non-zero readout coefficients against observed discrimination performance across participants under no cTBS and IPL cTBS in the intention discrimination task **(G)** and in the kinematic discrimination task **(H)**. The alignment index was highly correlated with task performance (top row). The correlation between individual task performance and the norm of the readout vector, which quantifies the level of internal decision noise for a given individual and thus the strength of readout for that individual [1], and the number of non-zero readout regression coefficients, which provides a measure of 'kinematic gathering', was much weaker (middle and bottom rows). We confirmed these results with a further stepwise regression to determine the relative importance of different model parameters for discrimination performance (Table S5).

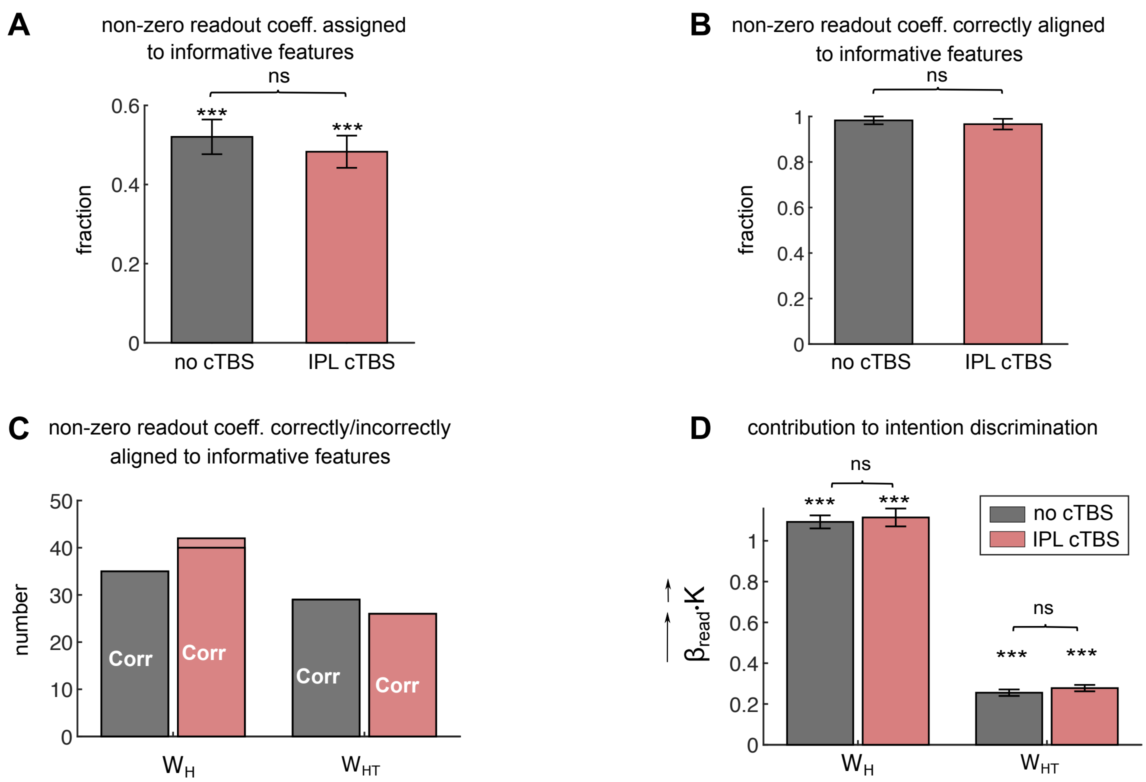

Figure S5. Quantification of alignment in the kinematic discrimination task. Related to Figure 5. (A) Fraction of non-zero readout coefficients assigned to informative features. **(B)** Fraction of non-zero readout coefficients assigned to informative features and correctly aligned with encoding. Fraction was computed on a subject basis and then averaged across subjects. **(C)** Number of non-zero readout coefficients (in)correctly aligned to informative features in encoding. We focused on the most informative and most read out kinematic variable: the height of the wrist (W_H) and the horizontal trajectory of the wrist (W_{HT}). **(D)** Contribution of W_H and W_{HT} to kinematic discrimination performance, computed as the scalar product between the kinematic vector and the readout vector within that feature subspace. Histograms represent mean ± SEM across all trials and participants.

	Left hemisphere		*Right hemisphere*	
ROI	*ACC*	*p value*	*ACC*	*p value*
IFG, all subareas	0.70	0.012	0.55	0.333
IFG pars triangularis	0.63	0.060	0.58	0.233
IFG pars orbitalis	0.73	0.006	0.43	0.853
IFG pars opercularis	0.70	0.002	0.60	0.114
IPL	0.78	0.001	0.65	0.030
Superior parietal lobule	0.70	0.005	0.65	0.034
Mid frontal gyrus	0.55	0.340	0.48	0.695
Precentral gyrus	0.58	0.210	0.55	0.284
Superior temporal gyrus	0.70	0.006	0.50	0.569
Inferior temporal gyrus	0.65	0.016	0.60	0.090
Supplementary motor area	0.65	0.039	0.58	0.202
Calcarine sulcus	0.78	0.001	0.70	0.004
Mid occipital	0.53	0.411	0.48	0.709
Inferior occipital gyrus	0.50	0.572	0.65	0.009

Table S1. MVPA results for AAL regions. Related to Figure 1. We trained and tested separate linear SVM classifiers to distinguish between intentions within each AAL ROI with accuracy assessed using leave-one-subject-out (LOSO) cross validation. Decoding accuracies and p values (1000 permutations) are reported for each ROI.

Intention discrimination task		Kinematic discrimination task	
Discrimination performance	***BIC***	***Discrimination performance***	***BIC***
Random intercept* *converged correctly*	355.540	Random intercept* *converged correctly*	393.939
Random intercept and slope *converged correctly*	366.601	Random intercept and slope *boundary (singular) fit*	406.100
Discrimination performance 10% trial selection	***BIC***	***Discrimination performance 10% trial selection***	***BIC***
Random intercept* *converged correctly*	215.415	Random intercept* *converged correctly*	206.278
Random intercept and slope *unable to evaluate scaled gradient*	226.079	Random intercept and slope *failed to converge with max|grad| = 0.00494831 (tol = 0.001, component 1)*	225.392
Response Bias	***BIC***	***Response Bias***	***BIC***
Random intercept* *converged correctly*	355.540	Random intercept* *converged correctly*	393.939
Random intercept and slope *converged correctly*	366.601	Random intercept and slope *boundary (singular) fit*	406.100
Contrast Discrimination	***BIC***	***Contrast Discrimination***	***BIC***
Random intercept* *converged correctly*	306.243	Random intercept* *converged correctly*	376.575
Random intercept and slope *boundary (singular) fit*	325.295	Random intercept and slope *failed to converge with max|grad| = 0.00608542 (tol = 0.001, component 1)*	393.328
Readout Model Performance	***BIC***	***Readout Model Performance***	***BIC***
Random intercept *converged correctly*	435.040	Random intercept* *converged correctly*	371.929
Random intercept and slope* *converged correctly*	383.088	Random intercept and slope *converged correctly*	379.901

Table S2. Comparison of the LMEMs tested for the selection of model's random-effect structure. Related to Figure 1. We selected the random-effect structure of the LMEM by comparing a random intercept only model (df 4) with a model including both random intercept and random slope (df 9). We performed model selection using the Bayesian Information Criterion (BIC), which rewards model fit and penalizes model complexity (number of df). Asterisks indicate retained models.

Intention discrimination task / Kinematic discrimination task

Task performance: comparison to chance (Figure 1D and 1E)

	Intention discrimination task					Kinematic discrimination task				
	Estimate	StdErr	z	d	p	Estimate	StdErr	z	d	p
NocTBS	0.314	0.102	3.069	0.767	0.006	1.459	0.123	11.834	2.715	<.001
IFG	0.279	0.102	2.730	0.682	0.013	1.462	0.123	11.855	2.720	<.001
IPL	0.072	0.102	0.708	0.177	0.479	1.295	0.122	10.621	2.437	<.001

Task performance: comparison across sessions (Figure 1D and 1E)

	Intention discrimination task					Kinematic discrimination task				
	Estimate	StdErr	z	d	p	Estimate	StdErr	z	d	p
NocTBS-IFG	-0.035	0.077	-0.455	-0.114	0.649	0.003	0.087	0.036	0.008	0.971
NocTBS-IPL	-0.242	0.076	-3.171	-0.793	0.005	-0.164	0.085	-1.927	-0.442	0.149
IFG-IPL	-0.207	0.076	-2.717	-0.679	0.013	-0.167	0.085	-1.963	-0.450	0.149

Task performance matching difficulty: comparison to chance (Figure S1C)

	Intention discrimination task					Kinematic discrimination task				
	Estimate	StdErr	z	d	p	Estimate	StdErr	z	d	p
NocTBS	0.657	0.243	2.697	0.674	0.021	0.747	0.165	4.537	1.041	<.001
IFG	0.558	0.242	2.310	0.578	0.042	0.720	0.164	4.395	1.008	<.001
IPL	-0.032	0.237	-0.134	-0.033	0.893	0.489	0.158	3.092	0.709	0.002

Task performance matching difficulty: comparison across sessions (Figure S1C)

	Intention discrimination task					Kinematic discrimination task				
	Estimate	StdErr	z	d	p	Estimate	StdErr	z	d	p
NocTBS-IFG	-0.098	0.255	-0.384	-0.096	0.701	-0.027	0.231	-0.116	-0.027	0.908
NocTBS-IPL	-0.688	0.253	-2.724	-0.681	0.019	-0.257	0.227	-1.132	-0.260	0.772
IFG-IPL	-0.590	0.251	-2.352	-0.588	0.037	-0.231	0.227	-1.017	-0.233	0.772

Readout model performance: comparison to chance (Figure 3D and 3G)

	Intention discrimination task					Kinematic discrimination task				
	Estimate	StdErr	z	d	p	Estimate	StdErr	z	d	p
NocTBS	1.129	0.146	7.752	1.938	<.001	2.067	0.115	17.976	4.124	<.001
IFG	1.194	0.160	7.456	1.864	<.001	2.113	0.116	18.234	4.183	<.001
IPL	0.987	0.137	7.200	1.800	<.001	2.027	0.114	17.740	4.070	<.001

Readout model performance: comparison across sessions (Figure 3D and 3G)

	Intention discrimination task					Kinematic discrimination task				
	Estimate	StdErr	z	d	p	Estimate	StdErr	z	d	p
NocTBS-IFG	0.066	0.229	0.286	0.072	0.908	0.046	0.107	0.428	0.098	1
NocTBS-IPL	-0.142	0.190	-0.749	-0.187	0.908	-0.040	0.106	-0.378	-0.087	1
IFG-IPL	-0.208	0.162	-1.283	-0.321	0.598	-0.086	0.107	-0.805	-0.185	1

Confidence ratings (high vs. low): comparison to chance

	Intention discrimination task					Kinematic discrimination task				
	Estimate	StdErr	z	d	p	Estimate	StdErr	z	d	p
NocTBS	0.005	0.191	0.025	0.006	1	0.342	0.120	2.852	0.654	0.004
IFG	-0.161	0.251	-0.640	-0.160	1	0.438	0.120	3.644	0.836	0.001
IPL	-0.029	0.165	-0.177	-0.044	1	0.418	0.120	3.479	0.798	0.001

Confidence ratings (high vs. low): comparison across sessions

	Intention discrimination task					Kinematic discrimination task				
	Estimate	StdErr	z	d	p	Estimate	StdErr	z	d	p
NocTBS-IFG	-0.166	0.185	-0.895	-0.224	1	0.096	0.071	1.339	0.307	0.542
NocTBS-IPL	-0.034	0.163	-0.208	-0.052	1	0.076	0.071	1.061	0.243	0.578
IFG-IPL	0.132	0.149	0.883	0.221	1	-0.020	0.072	-0.278	-0.064	0.781

Response bias: comparison to chance (Figure S1B)

	Estimate	StdErr	z	d	p	Estimate	StdErr	z	d	p
NocTBS	0.030	0.066	0.450	0.112	0.653	-0.060	0.055	-1.095	-0.251	0.689
IFG	0.097	0.066	1.459	0.365	0.434	-0.066	0.055	-1.201	-0.276	0.689
IPL	0.083	0.066	1.249	0.312	0.434	-0.056	0.055	-1.030	-0.236	0.689

Response bias: comparison across sessions (Figure S1B)

	Estimate	StdErr	z	d	p	Estimate	StdErr	z	d	p
NocTBS-IFG	0.067	0.075	0.893	0.223	1	-0.006	0.069	-0.085	-0.020	1
NocTBS-IPL	0.053	0.075	0.707	0.177	1	0.004	0.069	0.052	0.012	1
IFG-IPL	-0.014	0.075	-0.185	-0.046	1	0.009	0.069	0.137	0.031	1

Contrast task: comparison to chance

	Estimate	StdErr	z	d	p	Estimate	StdErr	z	d	p
NocTBS	1.627	0.124	13.110	3.277	<.001	1.493	0.102	14.636	3.358	<.001
IFG	1.512	0.123	12.295	3.074	<.001	1.460	0.102	14.368	3.296	<.001
IPL	1.646	0.124	13.236	3.309	<.001	1.511	0.102	14.797	3.395	<.001

Contrast task: comparison across sessions

	Estimate	StdErr	z	d	p	Estimate	StdErr	z	d	p
NocTBS-IFG	-0.115	0.096	-1.198	-0.299	0.494	-0.033	0.085	-0.393	-0.090	1
NocTBS-IPL	0.019	0.097	0.193	0.048	0.847	0.018	0.086	0.212	0.049	1
IFG-IPL	0.134	0.096	1.390	0.347	0.494	0.052	0.085	0.606	0.139	1

Task performance: comparison between blocks 1 and 2

	Estimate	StdErr	z	d	p	Estimate	StdErr	z	d	p
NocTBS	0.080	0.094	0.855	0.214	0.458	-0.022	0.106	-0.209	-0.048	1
IFG	0.145	0.094	1.545	0.386	0.367	-0.043	0.105	-0.413	-0.095	1
IPL	-0.112	0.093	-1.203	-0.301	0.458	-0.035	0.104	-0.338	-0.078	1

Main effects and interactions

	χ2	df	p	χ2	df	p
Main effect of session	11.79	2	0.003	5.06	2	0.080
Main effect of interval	12.13	3	0.007	18.70	3	<.001
Interaction of interval and session	0.35	2	0.838	0.04	2	0.978

Table S3. Summary of LMEM statistical tests. Related to Figures 1, 2 and 3. We tested the significance of fixed effects (see STAR Methods). Estimate, StdErr, z refer to the estimate of the effect, its standard error and the z value computed with the LMEM model using the R Package multcomp. d reports Cohen's *d* and p reports the two-sided p-value computed from the z test. All p values are Holm-Bonferroni corrected for the number of comparisons listed for each entry reporting each test. Tested main effects and interactions (computed as χ2 likelihood ratio tests of LMEM; see STAR Methods) are reported in the bottom entry.

	Intention discrimination task				Kinematic discrimination task			

Readout model performance: comparison to permuted data

	Value	StdPerm	z_perm	p	Value	StdPerm	z_perm	p
NocTBS	0.744	0.016	9.593	<.001	0.883	0.018	16.568	<.001
IFG	0.753	0.016	9.414	<.001	0.887	0.014	20.869	<.001
IPL	0.718	0.017	6.719	<.001	0.878	0.014	20.249	<.001

Norm of the readout vector: comparison across sessions

	Value	StdPerm	z_perm	p	Value	StdPerm	z_perm	p
NocTBS-IFG	0.211	0.393	0.530	0.748	-0.094	0.230	-0.427	1
NocTBS-IPL	0.414	0.395	1.045	0.758	-0.080	0.263	-0.312	1
IFG-IPL	0.203	0.171	1.195	0.758	0.014	0.303	0.052	1

Number of non-zero readout coefficients: comparison across sessions

	Value	StdPerm	z_perm	p	Value	StdPerm	z_perm	p
NocTBS-IFG	0.500	1.794	0.274	1	-2.000	1.345	-1.500	0.453
NocTBS-IPL	1.188	1.699	0.696	1	-1.632	1.130	-1.449	0.453
IFG-IPL	0.688	1.164	0.595	1	0.368	1.321	0.288	0.815

Alignment Index (all trials): comparison to encoding and across sessions (Figure 4E and S4D)

	Value	StdPerm	z_perm	p	Value	StdPerm	z_perm	p
NocTBS-Encoding	-0.117	0.005	-24.526	<.001	-0.048	0.004	-12.949	<.001
IFG-Encoding	-0.121	0.005	-25.463	<.001	-0.037	0.004	-10.068	<.001
IPL-Encoding	-0.140	0.005	-27.081	<.001	-0.038	0.004	-9.610	<.001
NocTBS-IFG	-0.006	0.006	-0.979	0.315	0.006	0.004	1.344	0.517
NocTBS-IPL	-0.021	0.006	-3.626	0.006	0.003	0.004	0.617	1
IFG-IPL	-0.015	0.006	-2.704	0.013	- 0.003	0.004	-0.652	1

Alignment Index (trials correctly predicted): comparison to encoding and across sessions (Figure S4E and S4F)

	Value	StdPerm	z_perm	p	Value	StdPerm	z_perm	p
NocTBS-Encoding	-0.110	0.006	-19.163	<.001	-0.037	0.004	-9.507	<.001
IFG-Encoding	-0.115	0.006	-20.735	<.001	-0.028	0.004	-7.170	<.001
IPL-Encoding	-0.137	0.006	-21.743	<.001	-0.028	0.004	-6.887	<.001
NocTBS-IFG	-0.005	0.006	-0.733	0.461	0.004	0.004	0.813	1
NocTBS-IPL	-0.025	0.007	-3.408	<.001	0.002	0.004	0.337	1
IFG-IPL	-0.020	0.007	-2.881	0.009	-0.002	0.005	-0.412	1

Non-zero readout coefficients assigned to informative features: comparison to chance (Figure 5A and S5A)

	Value	StdPerm	z_perm	p	Value	StdPerm	z_perm	p
NocTBS	0.402	0.147	2.71	0.010	0.52	0.148	3.5	<.001
IPL	0.35	0.159	2.19	0.039	0.42	0.124	3.3	<.001

Non-zero readout coefficients assigned to informative features: across sessions (Figure 5A and S5A)

	Value	StdPerm	z_perm	p	Value	StdPerm	z_perm	p
NocTBS-IPL	-0.044	0.063	-0.682	0.494	-0.037	0.047	-0.784	0.430

Non-zero readout coefficients aligned to informative features: across sessions (Figure 5B and S5B)

	Value	StdPerm	z_perm	p	Value	StdPerm	z_perm	p
NocTBS-IPL	-0.234	0.090	-2.639	0.007	-0.017	0.024	-0.699	0.754

Table S4. Summary of permutation tests. Related to Figures 4 and 5. Details of non-parametric permutation tests are described in STAR Methods. Value reports the actual value of quantity to be tested. The p value is computed comparing the actual value to the null-hypothesis distribution computed on permuted data. All p values are Holm-Bonferroni corrected for the number of comparisons listed for each entry reporting each test. For reference only, we also report (without using them to compute the p value) the standard deviation of the permuted values (StdPerm) and the actual value z-scored with this standard deviation (z_perm).

	Intention discrimination task			Kinematic discrimination task		
Pearson correlation between confidence and alignment						
	r	p		r	p	
NocTBS	0.044	0.242		0.335	< 0.001	
IFG	0.080	0.020		0.272	< 0.001	
IPL	-0.040	0.242		0.302	< 0.001	
Correlation between change in task performance and change in alignment						
	r	p		r	p	
NocTBS-IFG	0.67	0.005		0.67	0.002	
NocTBS-IPL	0.84	< 0.001		0.74	< 0.001	
IFG-IPL	0.83	< 0.001		0.75	< 0.001	
Correlation between task performance and trial number						
	r	p		r	p	
NocTBS	0.05	0.539		0.01	0.926	
IFG	0.07	0.431		0.01	0.906	
IPL	-0.12	0.164		-0.09	0.261	
Stepwise linear regression of log of ratios between IPL cTBS and no cTBS task performance						
	Coefficient	StdErr	p	Coefficient	StdErr	p
Alignment	4.031	0.811	< 0.001	3.811	0.676	< 0.001
Norm readout vector	-0.039	0.026	0.169	-0.096	0.027	0.003
N nonzero read coeff	-0.067	0.036	0.095	-0.045	0.028	0.138

Table S5. Summary of correlation and stepwise regression analyses. Related to Figure 4. Details of correlations and stepwise linear regression analyses are described in STAR Methods. All p values are Holm-Bonferroni corrected for the number of comparisons listed for each entry reporting each test. For stepwise linear regression analyses (bottom entry in the table), predictors (alignment index, norm of the readout vector and number of non-zero readout coefficients) are listed from top to bottom in terms of the importance imputed to them by the stepwise regression.

Supplemental References

S1. Norton, E.C., and Dowd, B.E. (2018). Log Odds and the Interpretation of Logit Models. Health Serv Res *53*, 859-878.